Published online 11 October 2017 *Nucleic Acids Research, 2017, Vol. 45, No. 22* **12723–12738**
doi: 10.1093/nar/gkx884

Rif1 promotes a repressive chromatin state to safeguard against endogenous retrovirus activation

Pishun Li[1,†], Li Wang[2,†], Brian D. Bennett[3], Jiajia Wang[1], Jialun Li[4], Yufeng Qin[1], Motoki Takaku[1], Paul A. Wade[1], Jiemin Wong[4] and Guang Hu[1,*]

[1]Epigenetics and Stem Cell Biology Laboratory, National Institute of Environmental Health Sciences, RTP, NC 27709, USA, [2]State Key Laboratory of Cardiovascular Disease, Fuwai Hospital, National Center for Cardiovascular Diseases, Chinese Academy of Medical Sciences and Peking Union Medical College, Beijing 100037, China, [3]Integrative Bioinformatics Support Group, National Institute of Environmental Health Sciences, RTP, NC 27709, USA and [4]Shanghai Key Laboratory of Regulatory Biology, Institute of Biomedical Sciences and School of Life Sciences, East China Normal University, Shanghai 200241, China

Received May 28, 2017; Revised September 14, 2017; Editorial Decision September 19, 2017; Accepted October 05, 2017

ABSTRACT

Transposable elements, including endogenous retroviruses (ERVs), constitute a large fraction of the mammalian genome. They are transcriptionally silenced during early development to protect genome integrity and aberrant transcription. However, the mechanisms that control their repression are not fully understood. To systematically study ERV repression, we carried out an RNAi screen in mouse embryonic stem cells (ESCs) and identified a list of novel regulators. Among them, Rif1 displays the strongest effect. Rif1 depletion by RNAi or gene deletion led to increased transcription and increased chromatin accessibility at ERV regions and their neighboring genes. This transcriptional de-repression becomes more severe when DNA methylation is lost. On the mechanistic level, Rif1 directly occupies ERVs and is required for repressive histone mark H3K9me3 and H3K27me3 assembly and DNA methylation. It interacts with histone methyltransferases and facilitates their recruitment to ERV regions. Importantly, Rif1 represses ERVs in human ESCs as well, and the evolutionally-conserved HEAT-like domain is essential for its function. Finally, Rif1 acts as a barrier during somatic cell reprogramming, and its depletion significantly enhances reprogramming efficiency. Together, our study uncovered many previously uncharacterized repressors of ERVs, and defined an essential role of Rif1 in the epigenetic defense against ERV activation.

INTRODUCTION

Transposable elements (TEs) comprise ∼50% of the mammalian genome. The vast majority of TEs are retrotransposons, which are mobile elements that spread by a copy-and-paste mechanism through reverse transcription and subsequent genome integration (1–4). Based on the structure, retrotransposons are divided into long terminal repeat- (LTR) and non-LTR elements. LTR retrotransposons closely resemble infectious retroviruses, and thereby are also called endogenous retroviruses (ERVs). They compromise ∼8% of the mouse genome, and can be subdivided into three families (ERV1, ERV2 and ERV3) according to the retroviruses they are derived from (5). ERVs can increase evolutionary complexity of their host via retrotransposition. In addition, they can serve as promoters or enhancers to modulate cellular gene activity during development (1,3,6,7). However, aberrant ERV transposition and activation often leads to genome instability and erroneous gene expression. Therefore, host mechanisms have evolved to restrict or limit ERV activities, especially in embryonic cells where ERV activation can have long term or even transgenerational effects (1–4). Interestingly, those mechanisms that control ERV activation also impinge on host gene expression (8–10). Thus, ERV regulation plays an integral role in shaping the gene expression program during development.

Repression of ERV transcription is the first step in controlling their activity, and it can be achieved by the repressive chromatin marks including DNA and histone methylations. DNA methylation at CpG dinucleotides, catalyzed by DNA methyltransferases (DNMTs), represses ERVs in somatic and germ cells (11,12). However, it has limited roles in embryonic stem cells (ESCs), as DNMT deletions only resulted in minimal ERV de-repression (13). On the other hand, histone methylations are the primary

*To whom correspondence should be addressed. Tel: +1 919 541 4755; Fax: +1 919 541 0146; Email: hug4@niehs.nih.gov
†These authors contributed equally to the paper as first authors.

mechanism for ERV silencing in ESCs (9,14). Both H3K9 dimethylation (H3K9me2) and trimethylation (H3K9me3), deposited by the EHMT1 and EHMT2 or the SETDB1 and SUV39H1/2 histone methyltransferases (HMTs), repress ERVs and other non-LTR retrotransposons (13,14). Specifically, EHMT1 and EHMT2 directly occupy and regulate ERV3 (15). SETDB1 represses ERV1 and ERV2 (13,14). SUV39H-dependent H3K9me3 marks and silences LINEs and intact ERVs (16). In addition to H3K9 methylations, H3K27 trimethylation (H3K27me3), deposited and maintained by the polycomb repressive complexes (PRCs), also plays a role in wild-type ESCs and becomes more important when DNA methylation is absent (9,17). Finally, other histone modifying enzymes, such as the histone demethylase KDM1A and the histone deacetylase HDAC1, have also been implicated in ERV silencing (18,19).

The establishment and maintenance of these repressive chromatin marks are mediated by DNA- or chromatin-associated factors. The best studied example is the universal co-repressor TRIM28. It is recruited by the Kruppel associated box containing zinc-finger (KRAB-ZnF) proteins to various retrotransposons, and promotes the deposition of repressive marks by recruiting DNMTs and HMTs (20–22). It can also be recruited to ERVs by the zinc-finger transcription factor YY1 (23). Besides TRIM28, the chromatin remodeling factor CHD5 was found to repress ERV3 by regulating H3K27me3 and histone variants H3.1/H3.2 (24). The histone chaperones CHAF1A/1B was identified in a RNAi screen to regulate different classes of ERVs via the interaction with histone modifying enzymes KDM1A, HDAC2 and SETDB1 (25).

To systematically dissect the role of epigenetic factors in ERV silencing, we carried out a RNAi screening in a MERVL (murine endogenous retrovirus with leucine tRNA primer)-LTR-driven tdTomato reporter mouse ESC line. We identified a list of novel ERV regulators, among which Rif1 shows the strongest impact. Rif1 was originally discovered as a factor involved in telomere length homeostasis in yeast (26). Later studies showed that Rif1 is also involved in DNA damage response (27–33), DNA replication timing (34–36), and epigenetic gene regulation (37). Furthermore, Rif1 is required for ESC maintenance (38,39), and its deletion leads to early embryonic lethality in the C57BL/6J strain (40). Here, we show that Rif1 depletion results in transcriptional de-repression of ERV and ERV-neighboring genes, and this de-repression becomes more obvious in DNA methylation deficient ESCs. Rif1 interacts with HMTs and facilitates their recruitment to ERVs, thereby promoting the establishment of repressive chromatin marks. We further show that Rif1 serves as a barrier during somatic cell reprogramming, and its transient depletion enhances induced pluripotent stem cell (iPSC) generation. Collectively, our study uncovers a list of novel ERV regulators and reveals an essential role of Rif1 in the transcriptional repression of ERVs.

MATERIALS AND METHODS

ESC culture and targeting

E14 and J1 ESCs were obtained from the American Type Culture Collection. Dnmt-TKO and Rosa26-CreERT2 ESCs were kindly provided by Dr Masaki Okano and Dr Shaun Cowley. For experiments, ESCs were routinely cultured on gelatin-coated plates in Dulbecco's modified Eagle's medium supplemented with 15% ESC-qualified fetal bovine serum, 10 mM 2-mercaptoethanol, 1 mM non-essential amino acids and 1000 U/ml of LIF (Millipore). For cell line maintenance, ESCs were cultured in the serum-free ESGRO medium (Millipore). ESC differentiation and transfections were carried out similarly as previously described (41).

For gene targeting, pX330 and homologous recombination (HR) donor plasmids were co-transfected into E14 (for HA-tag knock-in) or Rosa26 CreERT2 (for conditional deletion) ESCs. Transfected cells were seeded at colonal density, and individual colonies were picked and screened by polymerase chain reaction (PCR). Correctly targeted clones were amplified and re-screened to confirm genotype.

Plasmid construction, lentivirus preparation and shRNA screen

Primers and oligos used in this study were listed in Supplementary Table S4. For pLKO.1 shRNAs, complementary single-stranded oligos (Supplementary Table S1) were annealed and cloned as suggested by the RNAi consortium. Full length human Rif1 CDS is kindly provided by Dr Dongyi Xu. The Rif1 full length and truncation fragments were PCR amplified and cloned into the pCAG-IRES-Blastcidin vector. Rif1 shRNA was derived from pGIPZ (GE Dharmacon, Clone ID V3LMM_484629) and sub-cloned into the pHAGE vector (42). For CRISPR-medicated genome editing, guide RNAs were cloned into the pX330 vector as instructed. For HA-tag knock-in, the guide RNA was designed to target the exon-1 region. For conditional deletion, the guide RNAs were designed to target introns between exon-4/5 and exon-6/7. HR donor sequences were amplified by PCR and cloned into pCRBlunt II-TOPO (Life Technologies). All plasmids were confirmed by sequencing.

Lentivirus was prepared as described previously by transfecting 293T cells. Virus was harvested 48 h after transfection. For the shRNA screen, 2C::tdTomato reporter ESCs were transduced with shRNA lentivirus, selected for viral infection with 2 μg/ml puromycin and then analyzed for tdTomato fluorescence by FACS 4 days after virus infection. The shRNA against the firefly luciferase was used as non-target control. The Rif1-B shRNA was used for RNA-seq, chromatin immunoprecipitation (ChIP)-seq and ATAC-seq in the study.

Antibodies

Antibodies used in this study include: HA (C29F4, CST 3724), RIF1 (Santa Cruz SC-65191), EZH2 (CST 5246), SETDB1 (Santa Cruz sc-66884), H3K9me3 (Abcam ab8898), H3K4me3 (Active motif 39159), H3K27me3 (Active motif 39155), H3K9ac (Millipore 07-352), H3K27ac (Active motif 31933), Suv39H1 (CST 8729), EHMT2 (CST 3306).

Immunoprecipitation (IP)

E14 HA-Rif1 ESCs or 293T cells co-transfected with plasmids encoding HA-tagged Rif1 and histone modifying enzymes (V5-tagged Setdb1, EZH2 or Suv39h1, or flag-tagged EHMT2) were used for immunoprecipitation (IP). Cells were harvested and lysed with lysis buffer (150 mM NaCl, 50 mM Tris, 1%NP40, pH 8.0, 10 mM NaF, 1 mM Na3VO4, Roche ethylenediaminetetraacetic acid (EDTA)-free protease inhibitor, phenylmethylsulfonyl fluoride (PMSF)). IP was carried out using anti-HA (3F10, Roche 11815016001) Affinity Matrix, V5 antibody-coupled Dynabeads (Life Technologies) or Flag antibody-coupled magnetic beads (Sigma) overnight at 4°C. After IP, beads were washed with lysis buffer and bound proteins were eluted with LDS loading buffer (Life Technologies). All experiments were performed three or more times, and representative results were shown in the figures.

Subcellular fractionation

Chromatin isolation method was adapted from Mendez and Stillman (43). Briefly, harvested cells were washed with phosphate-buffered saline (PBS) and re-suspended in cytosolic buffer (10 mM HEPES [pH 7.4], 10 mM KCl, 1.5 mM MgCl2, 0.34 M sucrose, 10% glycerol, 1 mM Dithiothreitol (DTT)) supplemented with protease inhibitors at a concentration of 20-40 million cells/ml, and incubated on ice for 5 min. A total of 1% Triton-X 100 in Equal volume of cytosolic buffer was added to a final concentration of 0.1%, and the cells were mixed by gently pipetting and further incubated for 10 min on ice. A total of 10% of this total volume was taken to preserve a whole-cell extract fraction. Nuclei was pelleted by centrifugation at 1300 × *g* for 5 min at 4°C, and supernatant containing the cytoplasmic fraction was collected. Nuclei were washed once in cytosolic buffer, then lysed 10 min on ice in 1× volume chromatin extraction buffer (3 mM EDTA, 0.2 mM EGTA, 1 mM DTT) supplemented with protease inhibitors. Insoluble chromatin was pelleted by centrifugation at 1700 × *g* for 5 min at 4°C, and supernatant containing the nucleoplasm fraction was collected. The chromatin pellet was washed once with chromatin extraction buffer. All fractions were boiled in LDS loading buffer. All experiments were performed three or more times, and representative results were shown in the figures.

Western blot and immunofluorescence staining

Cells were lysed with lysis buffer (150 mM NaCl, 50 mM Tris, 1%NP40, pH 8.0, 10 mM NaF, 1 mM Na3VO4, PMSF, Roche EDTA-free protease inhibitor). Cell lysate was loaded into a NuPAGE® Bis-Tris gels (4–12%) or NuPAGE® Tris-Acetate gels (3–8%, for >250 KD large proteins) and transferred onto a PVDF or NC membrane. The membrane was blocked with 5% non-fat milk at room temperature for 1 h, followed by incubation with primary antibodies at 4°C overnight. The blot was subsequently incubated with either horse-radish peroxidase (HRP)-conjugated anti-mouse IgG, HRP-conjugated anti-rabbit IgG or HRP-conjugated anti-goat IgG (1: 10 000). Signal was detected using G:Box range of system (Synoptics Ltd).

Cells were fixed using 4% paraformaldehyde at room temperature for 15 min, followed by 0.5% Triton X-100 permeabilization for 10 min and 0.5% bovine serum albumin blocking for 30 min. They were then incubated with primary antibodies at 37°C for 2 h or 4°C overnight, followed by secondary antibodies (Life Technologies). Nuclei were counterstained with DAPI (Sigma), and images were taken on the X-Cite 120Q microscope (Excelitas Technologies Corp). All experiments were performed three or more times, and representative results were shown in the figures.

RNA isolation, reverse transcription, qPCR and RNA-seq

Total RNA were isolated from cells using the GeneJet RNA purification kit (Thermo Scientific), and 0.5 μg total RNA were reverse transcribed to generate cDNA using the iScriptTM cDNA Synthesis Kit (Bio-Rad) according to manufacturer's instructions. qPCRs were performed using the SsoFastTM EvaGreen Supermix (Bio-Rad) on the Bio-Rad CFX-384 or CFX-96 Real-Time PCR System. Actin was used for normalization. Primers used in the study were listed in Supplementary Table S4. All experiments were performed three or more times, and representative results were shown in the figures. For RNA-seq, libraries were prepared from two biological replicates using the TruSeq RNA Sample Prep Kit and sequenced on the NextSeq (Illumina).

Chromatin immunoprecipitation (ChIP) assay and high-throughput sequencing

ChIP was performed as described previously (44). Briefly, 70–80% confluency of ESCs were crosslinked with a final concentration of 1% formaldehyde for 10 min at room temperature, formaldehyde was quenched by the addition of 200 mM glycine and cells were rinsed twice with ice-cold PBS. Cells were transferred to 15 ml conical tubes and collected by centrifugation. Cells were lysed with lysis buffer A (50 mM HEPES-KOH (pH 7.5), 140 mM NaCl, 1 mM EDTA, 0.5% NP-40, 0.25% Triton X-100, 10% Glycerol and protease inhibitor cocktail (Roche)), incubated at 4°C for 10 min and collected by spinning at 1300 × *g* for 5 min at 4°C. Cells were then resuspended in lysis buffer B (10 mM Tris–Cl (pH 8), 200 mM NaCl, 1 mM EDTA, 0.5 mM EGTA and protease inhibitor cocktail), incubated at room temperature for 10 min. Nuclei were pelleted by spinning at 1300 × *g* for 5 min at 4°C. The pellet was suspended with lysis buffer B (10 mM Tris–Cl (pH 8), 100 mM NaCl, 1 mM EDTA, 0.5 mM EGTA, 0.1% Na-Deoxycholate, 0.5% N-lauroylsarcosine and protease inhibitor cocktail) and incubated for 15 min on ice. Chromatin shearing was conducted with cells on ice, using a microtip attached to Misonix 3000 sonicator. Sonicate 8–12 cycles of 30 s ON and 90 s OFF around 30-watt power-output. A final concentration of 1% Triton X-100 was added and gently mixed by pipetting. The chromatin solution was clarified by spinning at 20 000 *g* at 4°C for 30 min. Chromatin immunoprecipitation was performed with 3 μg Dynabeads protein G (Life technology) conjugated preliminary antibodies antibody overnight at 4°C. The immunoprecipitated material was washed five

times with wash buffer (10 mM Tris–Cl (pH 8), 1 mM EDTA, 0.5% NP40, 0.5M LiCl, 0.5% Na-Deoxycholate) and once with TE buffer (PH8.0), then, eluted by heating for 30 min at 65°C with elution buffer (50 mM Tris–Cl (pH 7.5), 10 mM EDTA, 1% sodium dodecyl sulphate). To reverse the crosslinks, samples were incubated at 65°C overnight, then the eluted was digested with a final concentration of 0.5 μg/ml RNasesA at 37°C, followed with a final concentrated of 0.5 μg/ml Proteinase at 55°C for 2 h. The immunoprecipitated DNA were then extracted with phenol chloroform isoamyl alcohol followed by chloroform, ethanol precipitated in the presence of glycogen and re-suspended in TE buffer. The resulting DNA was analyzed by qPCR and data were presented as the percentage of input using indicated primers (Supplementary Table S4). All experiments were performed three or more times, and representative results were shown in the figures. For ChIP-seq, 1 ng precipitated DNA or input was used to generate DNA library by use of Nextera XT DNA sample preparation Kit (illumina) according to the manufacturer's instruction. The resulting libraries were used for sequencing by Next-Seq (Illumina). Two biological replicates were performed here, and combined reads were used for further analysis.

Assay for transposase accessible chromatin with high-throughput sequencing (ATAC-seq)

ATAC-seq was performed as described (45). Briefly, the harvested cell pellet was resuspended in cold lysis buffer (10 mM Tris–Cl (pH 7.4), 10 mM NaCl, 3 Mm MgCl, 0.1%(V/V) Igepal CA-630) and placed on ice for 5 min. Then crude nuclei were pelleted by centrifuge for 5 min at 500 × *g*, 4°C. Nuclei pellet were resuspended in transposition mix (Illumia cat# FC-121-1030), then DNA were purified using a Qiagen MinElute PCR purification kit. ATAC-seq library was generated by PCR amplification and sequenced on the NextSeq (Illumina). Two biological replicates were performed here, and combined reads were used for further analysis.

Analysis of DNA methylation

DNA methylation by HPLC and bisulfite sequencing was performed as described (46). Briefly, ESCs were re-suspended with lysis buffer (10 mM Tris–Cl (pH 7.5), 10 mM EDTA, 10 mM NaCl, 0.5% sarcosyl, 1 mg/ml Proteinase K) and incubated at 60°C overnight. Genomic DNA was extracted by phenol/chloroform and ethanol precipitated. The samples were re-suspended in TE buffer with a final concentration of 0.1 mg/ml RNaseA and 2U/ml RNaseH1, followed by 65°C incubation for 10 min and 37°C for 2 h. The RNA-free genomic DNAs were purified by phenol/chloroform extraction followed by ethanol precipitation. A total of 10 μg genomic DNA was digested with digestion solution (20 mM NaAc (pH 5.3), 1 mM ZnSO4,10U/u1 nuclease P1 (Sigma)) at 37°C overnight and 10U CIP(NEB) for additional 2 h at 37°C. Twenty microliters of hydrolyzate were analyzed using a HPLC system (Agilent Technologies, 1200 Series), equipped with an Agilent Eclipse XDB-C18 column (5 mm, 4.6 250 mm, Agilent Technologies Inc.). Three biological replicates were performed.

For DNA dot blot, genomic DNA was denatured by heating at 95°C, immediately cooled on ice and loaded on Amersham Hybond-N+ membrane. After UV crosslinking, the membrane was blocked by 5% non-fat milk for 1 h at room temperature, then incubated with 5mC or 5hmC antibody for 1 h at room temperature. The blot was subsequently incubated with either horse-radish peroxidase (HRP)-conjugated anti-mouse IgG or HRP-conjugated anti-rabbit IgG (1:10 000). Signal was detected using G:Box range of system (Synoptics Ltd). Three biological replicates were performed, and a representative result was shown in the figures.

Bisulfite conversion was performed using EZ DNA Methylation-Gold™ Kit (ZYMO research) according to the manufacturer's protocol. Bisulfite-treated DNA was used to amplify the targeted region, amplified regions were cloned into pGEM®-T Easy Vector (Promega) and sequenced. The primers are listed in Supplementary Table S4.

For methylated DNA immunoprecipitation, genomic DNA was extracted with the DNeasy Blood &Tissue Kit (QIAGEN). One microgram of extracted DNA was sonicated using covaris s220 to a mean fragment size of 150 bp, and then used for methylated DNA immunoprecipitation using 5mC antibody (Active motif). Immunoprecipitated DNA was purified using MinElute PCR Purification Kit (QIAGEN), after which the sample was used for qPCR. The experiment was performed three or more times, and a representative result was shown in the figures.

Somatic cell reprogramming

Mouse embryonic fibroblasts (MEFs) were plated in 12-well plate at 200 k/well, and transduced with the non-targeting or Rif1 shRNA viruses the next day. Two days after transduction, cells were re-plated in 12-well plate at 80 k/well, and were transduced with the pHAGE-STEMCCA viruses (47) encoding the Yamanaka factors the next day (day-1). Cells were re-plated in gelatin-coated 12-well plates at 80 k/well at day-2. On day-3, culture medium was switched from MEF medium to ESC medium, and medium was changed every day until day-12. For transient Rif1 silencing, doxycycline was added to the medium on day-6 to day-8 and removed afterward. All experiments were performed three or more times, and representative results were shown in the figures.

Bioinformatics analysis

For all sequencing runs, reads were removed if they had a mean Phred quality score of <20. Adapter sequence was trimmed using cutadapt v1.11. RNA-seq reads were aligned using TopHat2 v2.0.4 with the following parameters: '–b2-sensitive –no-coverage-search -g 10′. ChIP-seq, MeDIP-seq and ATAC-seq reads were aligned using Bowtie v0.12.8 with the following parameters: '-v 2 -M 1 –best –strata'. The '-M 1′ parameter ensured that multi-mapped reads were not removed, but instead aligned to one of the positions chosen at random. For RNA-seq, FPKM values were obtained using Cufflinks v2.0.2 with a RefSeq gene model downloaded from the UCSC browser. For ATAC-seq, open chromatin coverage was generated using the first nine bases of

the aligned reads. For ChIP-seq, peaks were called using SICER with a window size of 200 and a gap size 600. Repeats were defined using RepeatMasker and download from their website: 'http://www.repeatmasker.org'.

Gene Set Enrichment Analysis (GSEA) was used to determine whether the Rif KD upregulated genes were enriched for genes that are specifically expressed at the 2-cell stage or during ZGA. To define the 2-cell stage genes, raw RNA-seq reads were downloaded for samples at various stages of mouse embryo development (from 1 cell to morula) from GEO (accession GSE44183) (48). Adapter was trimmed using cutadapt v1.11, and the reads were aligned using TopHat2 v2.0.4. FPKM values were generated using Cufflinks v2.0.2, and they were normalized using quantile normalization. For each gene, a 2C score was calculated from the normalized FPKM values as: mean(2C samples)-[mean(non-2C samples)+2*sd(non-2C samples)]. Genes were defined as 2C-specific if the 2C score was >0. Genes were removed if more than one of the 2C samples had an FPKM of less than 1. Gene set of ZGA genes was obtained from (49).

We used the following published datasets for analysis: Setdb1 (GSE18371, (10)); Suv39h1/2 (GSE57092, (16)); Trim28 (GSE41903, (50)); G9a (GSE46536, (51)); H3K27me3 (GSE28254, (52)); Chaf1a/1b and Setdb1 (GSE70863, (25)).

RESULTS

shRNA screen identified Rif1 as a negative regulator of ERV silencing in ESCs

To systematically study ERV silencing, we carried out an RNAi screen in ESCs. We generated an MERVL-LTR-driven 2C::tdTomato reporter ESC line based on the published strategy (49), in which the expression of ERV3 can be determined by the reporter activity (Supplementary Figure S1A). We verified that the tdTomato-positive cells show elevated MERVL expression by RT-qPCRs (Supplementary Figure S1B). Using the reporter cells, we screened selected epigenetic regulators and examined the impact of their silencing on ERV3 expression (Figure 1A). From the screen, we identified a number of factors that when depleted resulted in reporter activation, including those that have been previously shown to repress ERV such as Chaf1a, Chaf1b, Chd5, Ehmt2, Kdm1a and Yy1 (Figure 1B and C; Supplementary Table S1) (18,23–25). Interestingly, silencing Trim28 only mildly affected the reporter activity, while silencing Setdb1 had no significant effect (Supplementary Table S1). Because the 2C::tdTomato reporter was designed to represent ERV3 expression, this result is consistent with their known function in ERV repression (13,20), and is also consistent with the notion that different epigenetic factors may be responsible for the control of different ERV subclasses (13,15,16,25). Among the identified factors, Rif1 showed the strongest phenotype (Figure 1B and C; Supplementary Figure S1C), and we decided to further investigate its role in ERV silencing. To confirm the RNAi result, we generated a Rif1 conditional knockout (cKO) ESC line using CRISPR-mediated genome editing (Supplementary Figure S1D and E). Similar as Rif1 KD, Rif1 deletion resulted in the activation of the 2C::tdTomato reporter (Figure 1D). Together, our screen identified Rif1 as a crucial factor for ERV silencing.

To determine the consequence of Rif1 depletion, we performed RNA-seq after Rif1 KD. We found a total of 591 upregulated genes and 377 downregulated genes (fold change > 2, FDR < 0.05) (Figure 2A and Supplementary Table S2), suggesting that Rif1 largely functions as a repressor. There was no obvious changes in most of the pluripotency genes (Supplementary Figure S2A), suggesting that Rif1 KD did not affect ESC differentiation. Importantly, we noticed that the upregulated genes are highly enriched for two cell (2C) stage and zygotic genome activation (ZGA) genes (Figure 2B and Supplementary Figure S2B). It has been reported that ERVs can act as alternative promoters or enhancers to activate neighboring genes during early development. Consistent with that notion, we found that the Rif1 KD-induced 2C- and ZGA-specific genes are located in close vicinity to ERVs (Figure 2C). Further, Rif1 KD often resulted in co-activation of ERVs and their nearby genes (Figure 2D). Finally, we examined the effect of Rif1 depletion on ERVs. We found that Rif1 KD or deletion indeed led to significant de-repression of ERVs (Figure 2D and E; Supplementary Figure S2C), with a more pronounced effect on ERV3 that is largely driven by MERVL elements (Figure 2F and G).

Previous studies have revealed several negative regulators of ERVs, including Setdb1, Suv39h1/2, Ehmt2, Chaf1a/b and Trim28 (14–16,18,20). Unsupervised hierarchical clustering analysis showed that Rif1 KD shared significant similarity with Chaf1a/1b KD in TE expression (Figure 2G and Supplementary Figure S2D), suggesting that they may regulate TEs via similar mechanisms. In comparison, while Ehmt2 has also been shown to regulate ERV3 and 2C-specific genes (15), it does not cluster tightly with Rif1. In line with the clustering analysis, there are large overlaps in de-pressed ERVs between Rif1 KD and Chaf1a/1b KD (Supplementary Figure S2E). Moreover, Chaf1a KD in Rif1 deficient cells did not induce additional ERV activation based on the 2C::tdTomato reporter assay (Supplementary Figure S2F). Collectively, our data clearly indicated that Rif1 is required for the repression of ERVs, especially ERV1 and ERV3, in mouse ESCs. Finally, Dux was recently shown to activate MERVL and 2C-genes (53–55). We found that Rif1 KD resulted in an increase in Dux expression. To test whether Dux expression may account for the de-repression of ERVs after Rif1 deletion, we silenced Dux by RNAi in Rif1 cKO 2C::tdTomato-reporter ESCs (Supplementary Figure S2G). Dux KD only partially rescued the reporter activation caused by Rif1 depletion (Supplementary Figure S2H), suggesting that Rif1-mediated ERV de-repression may act through both Dux-dependent and independent mechanisms.

Rif1 facilitates the assembly of repressive histone marks and DNA methylation at ERVs

To test whether Rif1 may directly regulate ERVs, we tagged endogenous Rif1 with the HA-tag using CRISPR/Cas9-mediated genome editing (Supplementary Figure S3A), following a strategy that has been previously shown to pre-

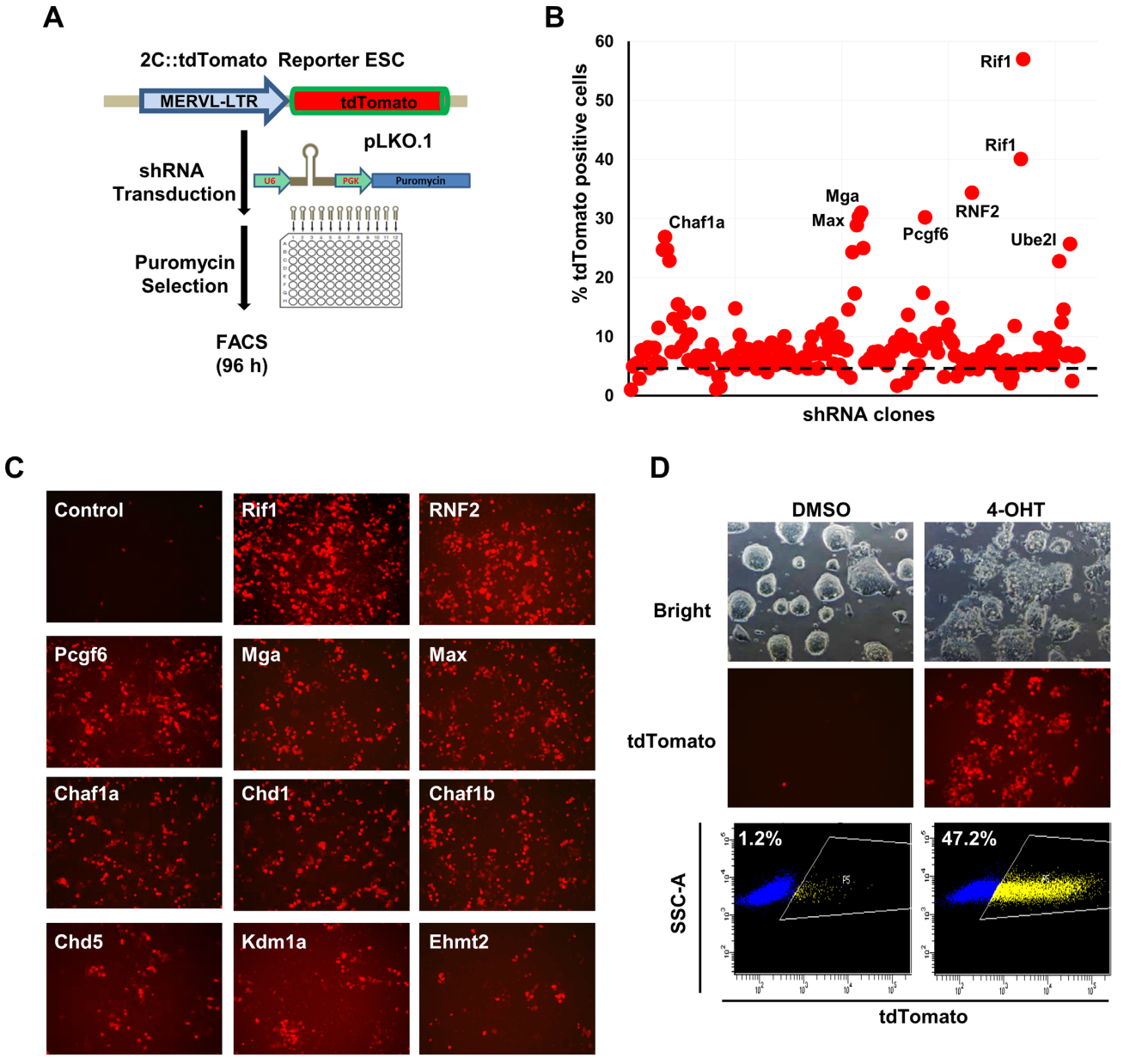

Figure 1. A shRNA screen identifies Rif1 as a negative regulator of ERVs. (**A**) Schematic of the shRNA screen. (**B**) Scatter plot showing the result of the shRNA screen. 2C::tdTomato reporter ESCs were transduced with shRNA lentiviruses, and the percentage of tdTomato-positive cell was determined by FACS at 96 h post-transduction. Black dotted line indicates 5% tdTomato-positive cells, and selected shRNAs were highlighted. (**C**) Representative images showing 2C::tdTomato reporter activity in ESCs transduced with top hits from the shRNA screen. (**D**) 2C::tdTomato reporter activation after Rif1 deletion. Rif1 conditional deletion ESCs were treated with DMSO or 4-OHT (0.1 μM) for 2 days, cultured for another two days without treatment, and then collected for imaging and FACS analysis.

serve Rif1 function (34). We confirmed the functionality of the inserted HA-tag by western blot and immunofluorescence staining (Supplementary Figure S3B and C). We then examined Rif1 genomic occupancy by chromatin immunoprecipitation followed by high-throughput sequencing (ChIP-seq) using an HA-antibody in this ESC line. We found that Rif1 occupies ERV1, ERV2 and ERV3s (Figure 3A and B; Supplementary Figure S3D, E and Table S3), suggesting that it may directly repress their expression. To validate this result, we carried out ChIP-qPCRs at selected ERV loci in Rif1 cKO ESCs treated with or without 4-hydroxytamoxifen (4OHT). We found that Rif1 occupancy was only detected in untreated but not treated cells in which Rif1 was deleted (Supplementary Figure S3F). In addition, we re-analyzed the Rif1 ChIP-seq data from a recent study (56), and confirmed Rif1 occupancy at ERVs (Supplementary Figure S3E).

Next, we examined histone H3 lysine 9 tri-methylation (H3K9me3) and histone H3 lysine 27 tri-methylation (H3K27me3) occupancy at RIF1-bound ERVs, as they play important roles in ERV repression. We found that different RIF1-bound ERV sub-families show different enrich-

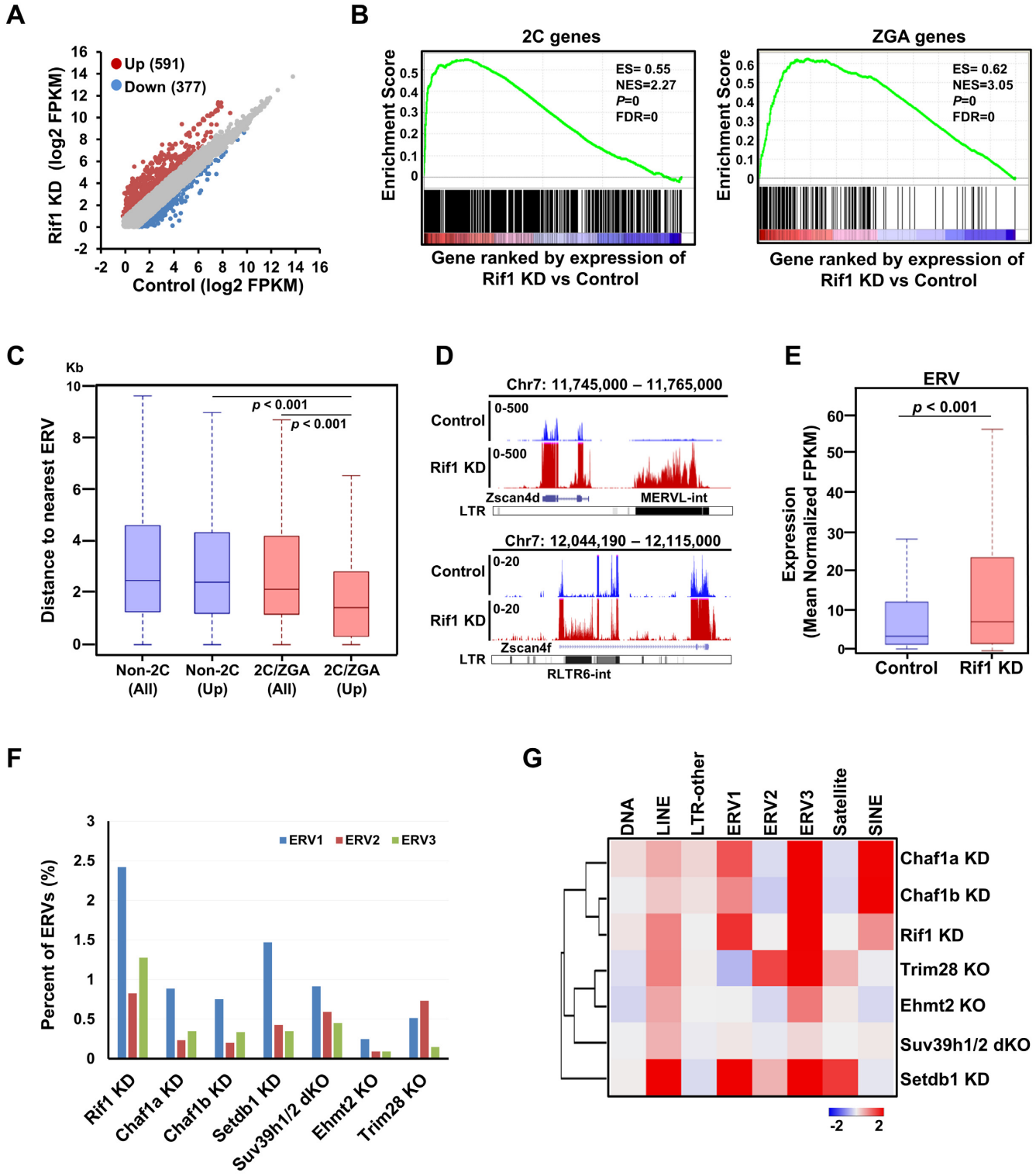

Figure 2. Rif1 depletion results in de-repression of ERVs and neighboring genes. (**A**) Scatter plot showing differentially expressed genes after Rif1 depletion (fold-change > 2 and FDR < 0.05). ESCs were transduced with luciferase (Control) or Rif1 shRNA (Rif1 KD) lentivirus, and cells were collected 96 h after transduction for analysis. (**B**) Gene set enrichment analysis (GSEA) showing that upregulated genes after Rif1 depletion are highly enriched for those that are specifically expressed at the 2-cell stage (2C genes) and during zygotic activation (ZGA genes). (**C**) Box plot showing the distance to the closest ERVs. 2C and ZGA genes were defined as described in the 'Materials and Methods' section. Non-2C and 2C/ZGA genes that were upregulated after Rif1 KD were compared to those that were not upregulated. *P*-value was calculated by Mann–Whitney Wilcoxon test. (**D**) Genome browser tracks showing elevated transcription of ERVs (MERVL-int and RLTR6-int) and neighboring genes (Zscan4d and Zscan4f) after Rif1 KD. *Y*-axis: normalized expression values of transcripts. (**E**) Box plot showing increased expression of ERVs after Rif1 KD. *P*-value was calculated by Mann–Whitney Wilcoxon test. (**F**) Column chart showing the regulation of ERV subfamilies upon depletion of the indicated factors. Percentage upregulated ERV in each subfamily was calculated as (number of upregulated ERV loci)/(number of total ERV loci). (**G**) Heat map showing the expression changes of repetitive elements upon the depletion of the indicated factors.

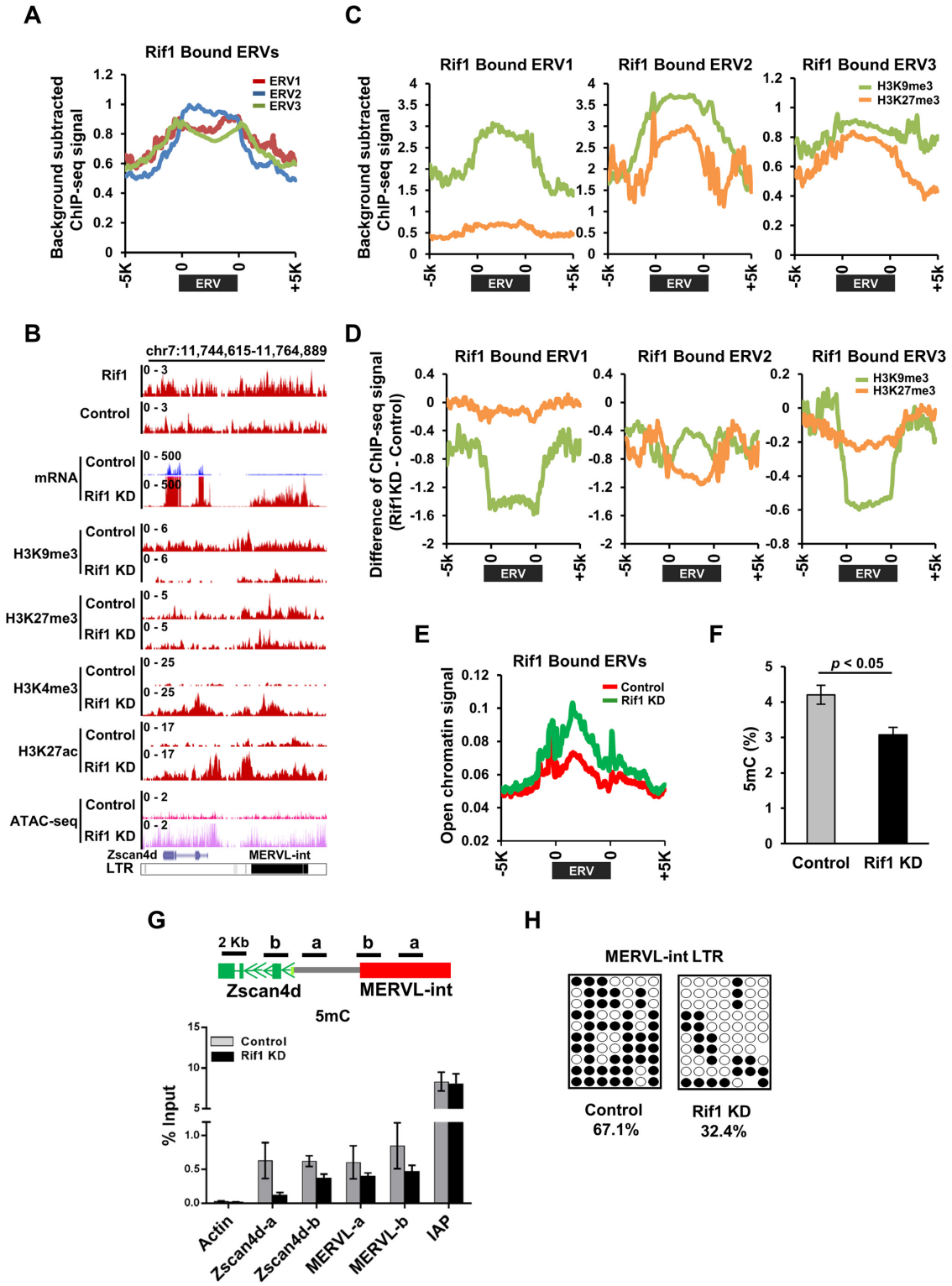

Figure 3. Rif1 occupies ERVs and regulates the chromatin state. (**A**) Metagene analysis showing Rif1 occupancy at ERV subfamilies. (B) UCSC genome browser tracks of mRNA expression, Rif1, H3K9me3, and H3K27me3 ChIP-seq and ATAC-seq signals at the MERVL-int and Zscan4d locus in Control and Rif1 KD ESCs. *Y*-axis, normalized expression values, ChIP-Seq or ATAC-seq signal. (**C**) Metagene analysis showing H3K9me3 and H3K27me3 occupancy at RIF1-bound ERVs. (**D**) Metagene analysis showing changes of H3K9me3 and H3K27me3 occupancy at RIF1-bound ERVs upon Rif1 KD. ESCs were transduced with luciferase (Control) or Rif1 shRNA (Rif1 KD) lentivirus, and cells were collected 96 h after transduction for analysis. (**E**) Metagene analysis showing chromatin accessibility determined by ATAC-seq at RIF1-bound ERVs in Control and Rif1 KD ESCs. (**F**) HPLC analysis of total DNA methylation in Control and Rif1 KD ESCs. *P*-value was calculated by Student's *t*-test. (**G**) MeDIP-qPCR showing changes in DNA methylation at the IAP, MERVL-int and Zscan4d locus in Control and Rif1 KD ESCs. % Input values were plotted as mean ± standard error. (**H**) Bisulfite sequencing showing changes in DNA methylation at the MERVL-int locus in Control and Rif1 KD ESCs.

ment for H3K9me3 and H3K27me3 (Figure 3C). To test whether Rif1 may regulate ERVs through these repressive histone marks, we first examined the global level of histone modifications in WT and Rif1 KD ESCs. Based on immunofluorescence and western blot, we found that Rif1 KD resulted in reduced H3K9me3 and H3K27me3 and increased H3K9ac and H3K27ac signals in the nucleus (Supplementary Figure S4A). Next, we performed histone mark ChIP-seq. While H3K27me3 occupancy was only modestly decreased, H3K9me3 occupancy at Rif1-occupied ERV1 and ERV3, but not ERV2, was significantly reduced after Rif1 KD (Figure 3B and D; Supplementary Figure S4B), consistent with the expression changes at these ERV subfamilies. Finally, Rif1 depletion increases the accessibility of newly packaged chromatin and chromatin-loop size (34,36). To test whether Rif1 also regulates chromatin at ERVs, we examined chromatin accessibility by assay for transposase-accessible chromatin with high throughput sequencing (ATAC-seq) (57), and found that Rif1 KD significantly increased genome accessibility around RIF1-bound ERV loci (Figure 3B and E). Together, our data suggested that Rif1 is required for the repression of ERVs, especially ERV1 and ERV3, likely by facilitating the assembly or maintenance of repressive histone marks. Further, although Rif1 shows similar occupancy at all three ERV subfamilies, Rif1 depletion selectively reduces H3K9me3 at ERV1 and ERV3, resulting in their de-repression. Our findings are consistent with previous reports that different H3K9 methylation-based mechanisms are utilized to silence different retrotransposon families (13–16,20,25).

In addition to histone modifications, DNA methylation also plays an important role in protecting repetitive elements from aberrant transcription, and rapid loss of DNA demethylation in ESCs can result in de-repression of retrotransposons (17). We found that Rif1 KD led to a reduction in global (Figure 3F) DNA methylation with a concomitant increase in global 5-hydroxymethylcytosine level (Supplementary Figure S4C). More importantly, based on MeDIP-qPCR and bisulfite sequencing, DNA methylation at the ERV MERVL is significantly reduced in Rif1 KD ESCs (Figure 3G and H). In comparison, Rif1 KD did not impact methylation at the IAP elements in the ERV2 subfamily (Figure 3G). Thus, in addition to repressive histone marks, Rif1 also promotes DNA methylation at ERVs, especially at ERV3s.

Rif1 plays a critical role in ERV repression in the absence of DNA methylation

H3K27me3 was recently shown to repress ERV during rapid DNA methylation loss (17). Because Rif1 regulates H3K27me3 occupancy at ERVs, we hypothesized that Rif1 may be critically required for ERV silencing in the absence of DNA methylation. We tested the impact of Rif1 depletion in WT and DNA methyltransferase triple knockout (Dnmt-TKO) ESCs. Dnmt-TKO alone had little impact on the examined ERVs, consistent with the literature (13). However, Rif1 depletion resulted in a more robust increase in ERV1 (GLN, MLV, RLTR6) and ERV2 (MMERVK10C, MusD) expression in Dnmt-TKO cells (Figure 4A). Next, we tested whether Rif1-mediated H3K27me3 is responsible for ERV silencing in the absence of DNA methylation. As previously reported (17,58), we observed an increase in global H3K27me3 level (Figure 4B), as well as specific H3K27me3 occupancy at ERVs in Dnmt TKO ESCs (Figure 4C and D). In addition, ERVs are activated when Eed, a core component of the PRC2 complex that deposits H3K27me3, was silenced (Figure 4E). Finally, Rif1 depletion resulted in reduced global H3K27me3 level (Figure 4B) and H3K27me3 enrichment at Rif1-regulated ERVs significantly (Figure 4F). Taken together, these data suggested that Rif1-mediated H3K27me3 deposition plays a critical role in ERV repression in the absence of DNA methylation.

Rif1 interacts with repressive HMTs and facilitates their recruitment

To understand how Rif1 facilitates the assembly of repressive histone marks at ERVs, we first examined whether Rif1 may regulate the expression of related HMTs. We found that Rif1 deletion did not lead to significant decreases in their expression, except for Ehmt2 (Supplementary Figure S5A and B). We next tested whether Rif1 may regulate the recruitment of the HMTs to ERVs. Using the Rif1-HA knock-in ESCs, we found endogenous Rif1 interacts with both H3K9- and H3K27-methyltransferase SETDB1, EHMT2, SUV39H1 and EZH2 (Figure 5A). In addition, we transfected 293Ts with plasmids expressing tagged Rif1 and Setdb1, Ezh2, Ehmt2 or Suv39h1 proteins, and detected interactions between Rif1 protein and these HMTs by co-immunoprecipitations (Supplementary Figure S5C and D). These results are largely in agreement with a recent report (37).

Analysis of published ChIP-seq data showed that SETDB1 and SUV39H1/2 are enriched at RIF1-bound ERV1 and ERV2, while SETDB1, SUV39H1/2 and EHMT2 are only modestly enriched at ERV3 (Supplementary Figure S5E). This is consistent with the lower H3K9me3 level at ERV3 (Figure 3C), and suggest that ERV3 repression is particularly sensitive to H3K9me3 regulation. To test the impact of Rif1 depletion on HMT occupancy, we carried out ChIP-qPCR for SETDB1, EHMT2, Suv39H1 and EZH2 in Control versus Rif1 KD or Rif1 KO ESCs. As previously reported (15,59), we found that SETDB1 was enriched at MLV (ERV1) and IAPEz, MMERVK10C, MusD (ERV2); EHMT2 was enriched at all of the tested ERVs; Suv39H1 was enriched at RTRL6 (ERV1), and IAPEz, MMERVK10C, MusD (ERV2); and EZH2 was enriched at MLV, RLTR6 (ERV1), MMERVK10C (ERV2) and MERVL (ERV3) in control ESCs (Figure 5B and C). Importantly, we found that Rif1 KD or KO resulted in reduced SETDB1, EHMT2, Suv39H1 and EZH2 binding at many of the tested ERVs (Figure 5B and C). In particular, both EHMT2 and Suv39H1 occupancy at MERVL was significantly decreased (Figure 5C). This result is consistent with the decreased level of H3K9me3 and H3K27me3 at these ERVs upon Rif1 KD. Furthermore, it provides a plausible explanation for the regulation of ERV3 by Rif1, as EHMT2 and Suv39H1-dependent H3K9 methylation are critical for ERV3 repression (15,16). Collectively, our data strongly suggested that

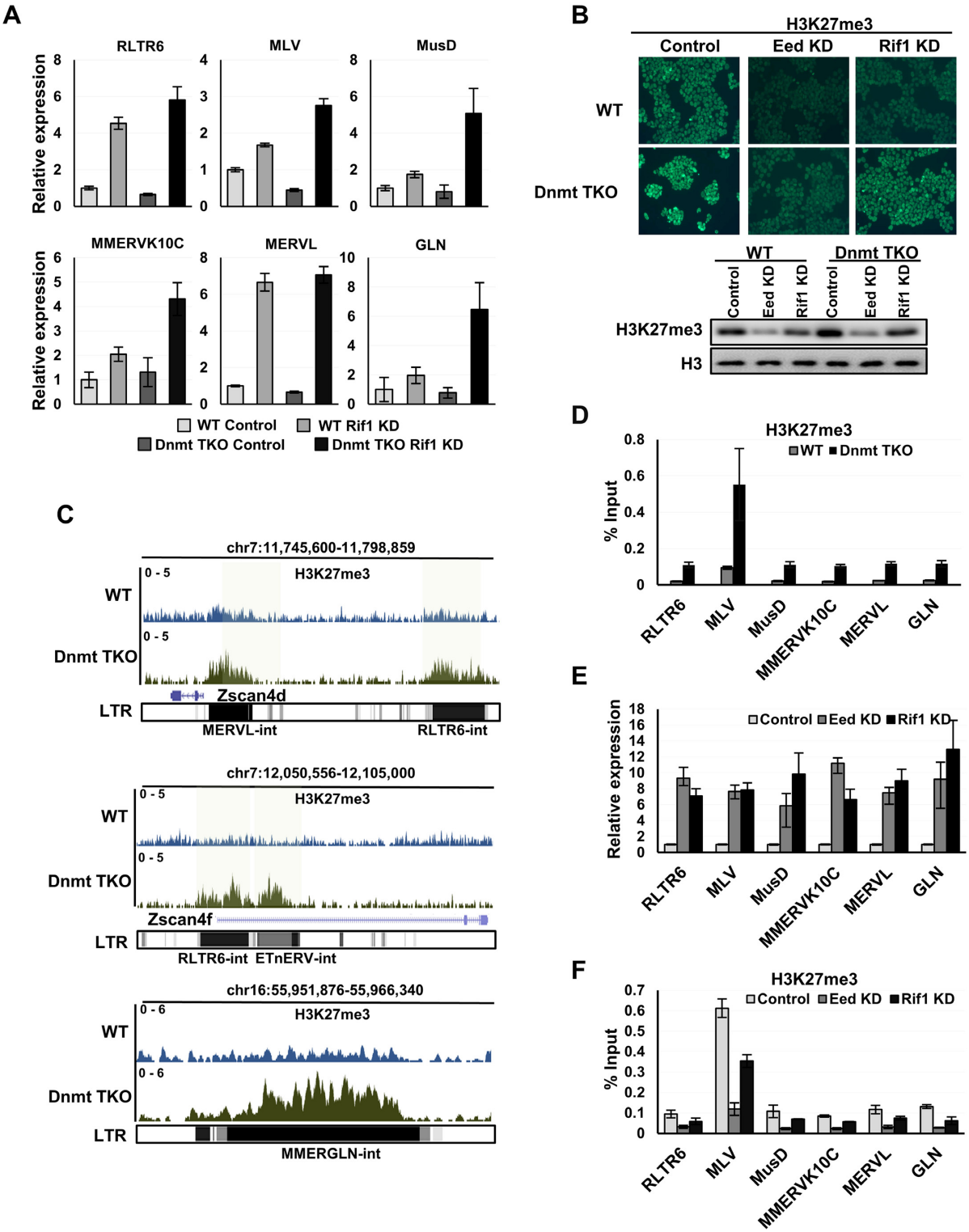

Figure 4. Rif1 is required for ERV repression in the absence of DNA methylation. (**A**) RT-qPCRs showing the upregulation of ERVs upon Rif1 KD in WT and Dnmt TKO ESCs. Relative expression values were normalized by Actin and plotted as mean ± standard error. (**B**) Immunofluorescence staining (up) and western blot (down) showing H3K27me3 level in WT and Dnmt TKO ESCs upon Eed or Rif1 KD. (**C**) Genome browser tracks showing H3K27me3 occupancy at ERV loci in WT and Dnmt TKO ESCs. Y-axis, normalized ChIP-Seq signal. (**D**) ChIP-qPCRs showing H3K27me3 occupancy at selected ERVs in WT and Dnmt TKO ESCs. % input values were plotted as mean ± standard error. (**E**) RT-qPCRs showing ERV expression in Dnmt TKO ESCs transduced with luciferase (Control), Rif1 shRNA (Rif1 KD), or Eed shRNA (Eed KD) lentivirus. ESCs were collected 96 h after transduction for analysis. Relative expression values were normalized by Actin and plotted as mean ± standard error. (**F**) ChIP-qPCRs showing H3K27me3 occupancy at selected ERV subfamilies in Dnmt TKO ESCs transduced with luciferase (Control), Eed (Eed KD) or Rif1 (Rif1 KD) shRNA lentivirus. ESCs were collected 96 h after transduction for analysis. % Input values were plotted as mean ± standard error.

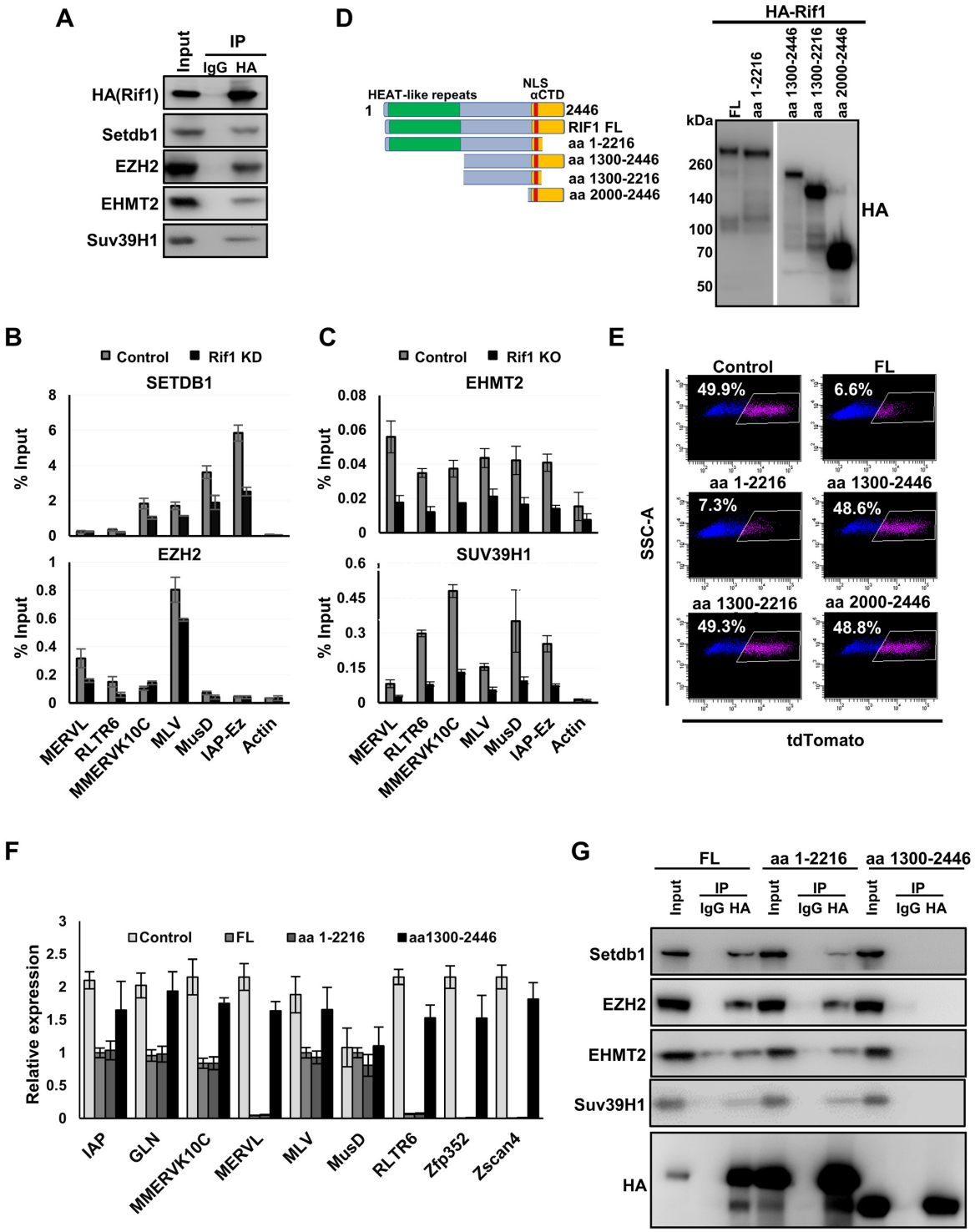

Figure 5. Rif1 interacts with HMTs and facilitates their recruitment at ERVs. (**A**) IP-western showing the interaction between RIF1 and SETDB1, EHMT2, SUV39H1 or EZH2. (**B** and **C**) ChIP-qPCRs showing SETDB1, EHMT2, SUV39H1 or EZH2 occupancy at RIF1-bound ERVs in Control, Rif1 KD or Rif1 KO ESCs. (B) For Rif1 KD, ESCs were transduced with luciferase (Control), or Rif1 shRNA (Rif1 KD) lentivirus, and cells were collected 96 h after transduction for ChIP. (C) For Rif1 KO, Rif1 cKO ESCs were treated with DMSO (Control) or 0.1 μM 4-OHT for 48 h, and cells were collected at 96 h for ChIP. % Input values were plotted as mean ± standard error. (**D**) Schematic representation of Rif1 domain constructs and western blots showing their expression in Rif1-cKO ESCs. (**E**) FACS analysis showing % 2C::tdTomato-positive cells in Rif1-cKO ESCs expressing different Rif1 domain constructions. ESCs were treated with 4-OHT (0.1 μM) for 2 days, cultured for another 2 days without treatment and then collected for analysis. (**F**) RT-qPCRs showing the expression of ERVs and 2C genes in Rif1-cKO ESCs expressing different Rif1 domain constructions. Relative expression values were normalized by Actin and plotted as mean ± standard error. ESCs were treated with 4-OHT (0.1 μM) for 2 days, cultured for another 2 days without treatment and then collected for analysis. (**G**) IP-western showing the interaction between Rif1 domains and SETDB1, EHMT2, SUV39H1 or EZH2 in ESCs.

Rif1 facilitates the recruitment of repressive histone modifying enzymes to repress ERV expression.

Rif1 contains two functional domains: the HEAT-like (Huntingtin, Elongation factor 3, A subunit of protein phosphatase 2A and Tor1) repeats and the C-terminal domain (CTD) (Figure 5D). To identify the functional domain(s) in Rif1, we carried out structure-function analysis. We expressed full-length Rif1 or various domain constructs (Figure 5D) in Rif1 cKO 2C::tdTomato ESCs. We verified that all the constructs were properly expressed and the resulting protein products maintain proper nuclear localization and chromatin association (Figure 5D; Supplementary Figure S5F and G). Remarkably, exogenous expression of both full length Rif1 and Rif1 with a-CTD domain deletion (aa 1-2216) largely rescued the Rif1 KO phenotype based on the reporter activity (Figure 5E). The expression of ERVs and their nearby genes were also rescued (Figure 5F). In contrast, exogenous expression of Rif1 without the HEAT-like repeat domain (aa 1300-2446, 1300-2216 or 2000-2446) had little effect (Figure 5E and F). The HEAT-like repeat domain is required for the interactions between Rif1 and SETDB1, EHMT2, Suv39H1 or EZH2 (Figure 5G), and the truncation mutant (aa 1-2216) occupies similar genomic regions as full-length Rif1 (Supplementary Figure S5H). Therefore, these results supported our model that Rif1 represses ERVs by promoting the recruitment of repressive HMTs. Notably though, the ChIP-seq signal from the truncation mutant is reduced compared to that of the wild-type Rif1 (Supplementary Figure S5H), suggesting that the C-terminal domain may still influence Rif1 binding to the genome to some extent.

Importantly, the structure function analysis was carried out using the human Rif1 gene. Further, the HEAT-like repeat domain is highly conserved across species (60). Consequently, we asked whether that Rif1's function in ERV repression is also conserved in human cells. Indeed, we found that Rif1 silencing resulted in ERV transcriptional activation in human ESCs (Supplementary Figure S5I and J). Thus, Rif1 represses ERV in different species, as well as in different types of pluripotent stem cells.

Rif1 serves as a barrier during somatic cell reprogramming

Previous reports suggested that the dynamic regulation of ERV expression may contribute to the reprogramming process (61,62). In line with that, ERV regulators were found to influence induced pluripotent stem cell (iPSC) generation (63–65). We first confirmed that ERVs such as MERVL and IAP, are gradually upregulated during the course of reprogramming (Figure 6A). To test whether Rif1 regulates reprogramming, we selected an shRNA that modestly reduced Rif1 expression in MEFs without changing the growth rate (Supplementary Figure S6A and B). We found that limited Rif1 silencing resulted in a small but significant enhancement in reprogramming efficiency, as demonstrated by the increased number of alkaline phosphatase-positive colonies and increased percentage of Oct4-GFP-positive cells (Figure 6B and C). Consistently, endogenous pluripotency markers Oct4, Sox2 and Nanog were more abundantly expressed in the cell population that was transduced Rif1 shRNA (Figure 6D). The effect of Rif1 silencing was even more obvious when only three factors (Oct4, Klf4 and Sox2) were used for reprogramming (Supplementary Figure S6C and D). Interestingly, Rif1 KD did not significantly increase the population of SSEA-1-positive cells at day 6 (Supplementary Figure S6E), suggesting that Rif1 likely acts at a later stage of reprogramming. To test that, we used a doxycycline-inducible shRNA expression system for stage-specific Rif1 silencing (Supplementary Figure S6F). We added doxycycline between day 6 and 8 of reprogramming, and then measured the population of Oct4-GFP cells at day 12. Markedly, transient Rif1 silencing from day 6 to 8 dramatically enhanced reprogramming efficiency, as shown by the increased percentage of Oct4-GFP positive cells (Figure 6E). Therefore, these results indicated that Rif1, and possibly Rif1-mediated ERV regulation, is a novel barrier during somatic cell reprogramming.

DISCUSSION

Retrotransposons increase evolutionary complexity of their host. However, they also present fatal threats if not properly controlled. Correspondingly, transcriptional activation of retrotransposons is tightly restricted through multiple repressive epigenetic mechanisms. In this study, we screened a list of known epigenetic regulators and identified many novel factors involved in ERV silencing. Among those, we showed that Rif1 represses ERVs, likely via the recruitment of HMTs to establish repressive chromatin marks. Further, Rif1-mediated ERV silencing also serves as a roadblock during somatic cell reprogramming.

Rif1 is a multifunctional gene. Its product was first identified as a telomere-binding protein in yeast that negatively regulates telomere length (26). Recent studies showed that it also plays important roles in DNA damage response and DNA replication timing (18,27,31,35,36,56). However, Rif1 has long been implicated in heterochromatin regulation in both yeast and mammalian cells (37,66–68), suggesting that it may have other conserved functions. Indeed, the Rif1 homologue from drosophila does not fully complement yeast or mammalian Rif1 function in DNA damage response (69). More intriguingly, drosophila telomeres are maintained by retrotransposons (70). As a result, drosophila does not have telomerase and many other telomere-associated proteins. However, drosophila Rif1 is phylogenetically very close to that of vertebrates (60). Combined with our findings, we propose that Rif1 likely adopted a critical function in retroviral silencing via the establishment of repressive chromatin marks during evolution, and its function in modulating the activity of repetitive elements may be conserved across higher species. In support of this notion, we showed that the broadly conserved HEAT repeat-domain in Rif1 is required for ERV silencing (Figure 5E–G), and Rif1 represses ERV in both mouse and human ESCs (Supplementary Figure S5I and J).

A handful of factors have been shown to repress ERVs in ESCs, albeit to different extent on different ERV subfamilies. For example, the universal transcriptional co-repressor Trim28 mediates the silencing of all classes of ERV, although it its repression on ERV3 may be a consequence of indirect effects (15). The H3K9 methyltransferase Setdb1 regulates ERV1 and ERV2 (13,14), but Suv39h1/Suv39h2

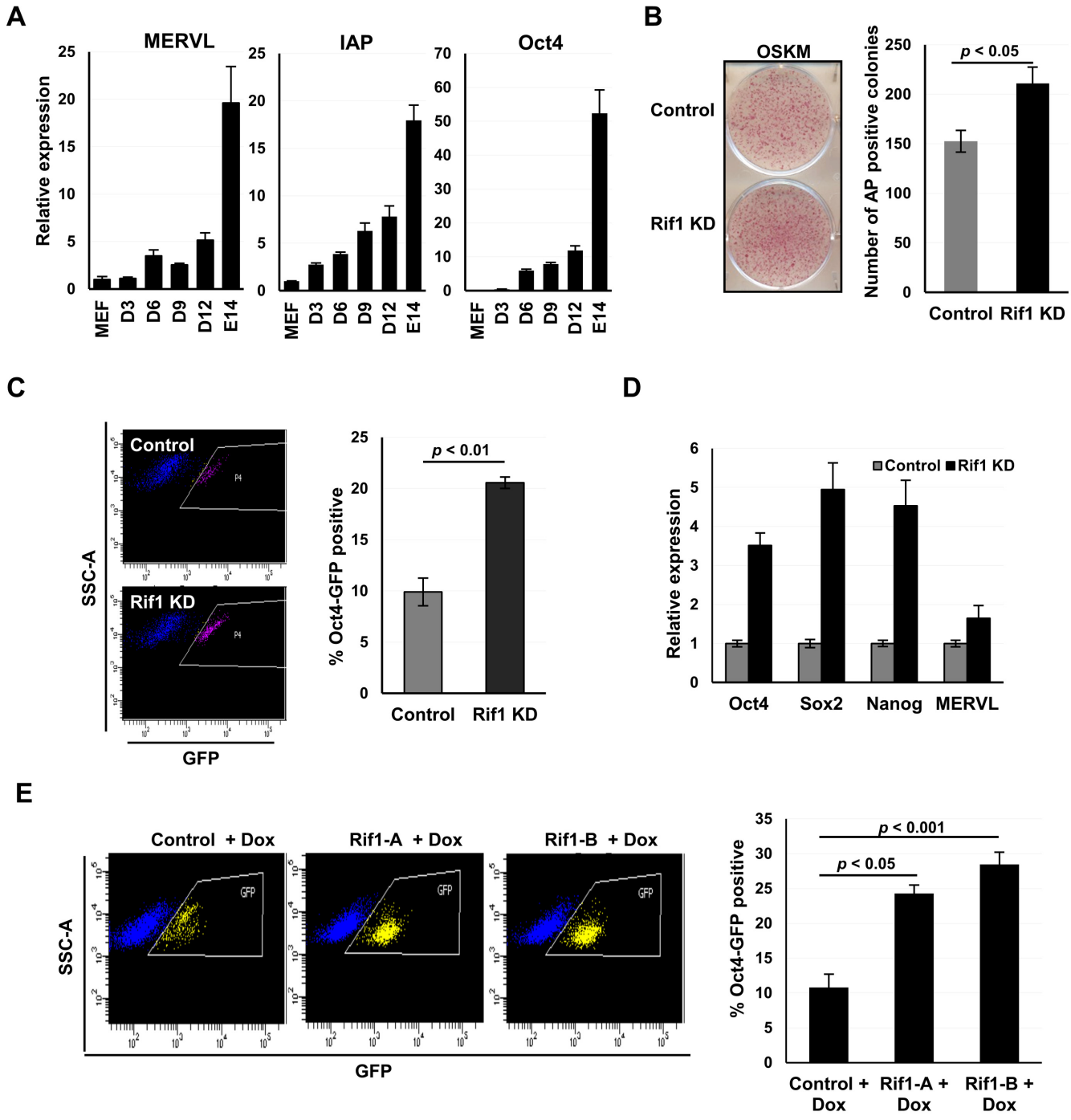

Figure 6. Rif1 acts as a barrier in somatic cell reprogramming. (**A**) RT-qPCRs showing ERV expression during reprogramming. Relative expression values were normalized by Actin and plotted as mean ± standard error. (**B**) AP-staining showing the impact of Rif1 silencing on reprogramming. MEFs were transduced with Rif1 shRNA lentivirus, and then with lentivirus expressing Oct4, Sox2, Klf4, Myc to induce reprogramming. Left: representative images of AP-positive cells; Right: number of AP-positive colonies after days (plotted as mean ± standard error). *P*-value was calculated by Student's *t*-test. (**C**) FACS analysis showing the % Oct4-GFP-positive cells after reprogramming. MEFs were transduced with Rif1 shRNA lentivirus, and then with lentivirus expressing Oct4, Sox2, Klf4 and Myc to initiate reprogramming (day-1). % Oct4-GFP-positive cells were determined by FACS at day-12. Left: representative FACS result; Right: statistics of % Oct4-GFP-positive cells (plotted as mean ± standard error). *P*-value was calculated by Student's *t*-test. (**D**) RT-qPCRs showing the expression of endogenous Oct4, Sox2, Nanog and MERVL at day-12 from (C). Relative expression values were normalized by Actin and plotted as mean ± standard error. (**E**) FACS analysis showing the % Oct4-GFP-positive cells after reprogramming. MEFs were transduced with control of Rif1 doxycycline-inducible shRNA lentivirus, and then with pHAGE-STEMCCA virus expression Oct4, Klf4, Sox2 and Myc to initiate reprogramming. Cells were treated with doxycycline from day-6 to day-8 after pHAGE-STEMCCA transduction, and % Oct4-GFP-positive cells were determined by FACS on day-12. Left: representative FACS result; Right: statistics of % Oct4-GFP-positive cells (plotted as mean ± standard error). *P*-value was calculated by Student's *t*-test.

predominantly affects intact ERVs and LINE elements (16). The histone demethylase Kdm1a and the polycomb complexes repress ERV3 (9,18). We identified Rif1 using the 2C::tdTomato-reporter assay. Consistently, we found that Rif1 depletion led to significant upregulation of ERV3 (Figure 2F and G), as the reporter was designed to faithfully recapitulate ERV3 expression. In comparison, silencing of the other known retrotransposon repressors mentioned above showed much reduced impact in the same assay, suggesting that Rif1 is a master regulator of this ERV subfamily. Interestingly, Rif1 was shown to interact with the histone chaperone Chaf1a (25), and our results further suggested that Rif1 and Chaf1a/1b may co-regulate ERV3 via shared mechanisms or pathways.

Mechanistically, we found that Rif1 occupies ERVs, interacts with multiple HMTs and promotes the establishment of multiple repressive chromatin marks, including H3K9me3, H3K27me3 and DNA methylation. H3K9 methylation is the main controller of retrotransposon activity in ESCs. DNA methylation also plays an important role, and H3K27me3 is required when DNA methylation is lost (17). Our findings indicated that Rif1 can ensure proper ERV silencing in different contexts, and uncovered novel mechanisms by which Rif1 can function as an epigenetic repressor (37). In addition, Rif1 not only facilitates H3K9me3 and H3K27me3 occupancy at ERVs, it has also been identified to interact with the histone marks (71), either directly or indirectly via Chaf1a. Therefore, Rif1 can potentially form a positive feedback with repressive histone modifications to engage ERV repression. Consistent with this notion, Rif1 silencing showed the strongest effect in ERV de-repression in our RNAi screen, even more so than the silencing of individual repressive HMTs alone (Supplementary Table S1). Besides repressive histone marks, RIF1 was recently found to interact with histone variants H3.1 and H3.2 (72). H3.1/3.2 deposition by Chaf1a/1b is associated with repressive histone marks at retrotransposons in pre-implantation embryos (73). These findings can potentially explain the similarities between Rif1 and Chaf1a/1b KD, and suggest another possible mechanism in which Rif1 represses ERVs by promoting Chaf1a/1b-mediated histone variant deposition. Together, we propose that Rif1 may act as a hub and integrate multiple repressive histone modifying enzymes and repression mechanisms to silence ERVs.

ERVs provide a rich reservoir of regulatory elements in the genome. In addition, ERV-containing sequences are metastable due to its epigenetic regulation and can promote variable expression of surrounding genes, resulting in phenotypic mosaicism and diversity. Indeed, ESCs display transcriptional heterogeneity of pluripotency-associated genes and ERVs, and their developmental capacity fluctuates with ERV activity (49,74). We found that Rif1 is required for the repression of both ERVs and many ERV-neighboring genes. In particular, its depletion resulted in a significant elevation of Zscan4. Zscan4 is transiently expressed in a subpopulation of ESCs, but is required for the long-term maintenance of the bulk population (74). Its expression marks a distinct epigenetic state, and promotes the rejuvenation of ESC potency (75,76). Thus, it is possible that Rif1 and Rif1-mediated epigenetic regulation plays an important role in regulating the maintenance and developmental potential of ESCs. Intriguingly, Zscan4 silencing can partially rescue the growth defect caused by Rif1 knockdown (37), possibly because they can both regulate telomere and genomic stability (28,74). However, it is unclear whether Zscan4 also plays a role in Rif1-dependent ERV repression.

Finally, it has been shown that retrotransposons are derepressed during somatic cell reprogramming. Moreover, transcription triggered by specific retrotransposons mediates and may even be an essential step toward iPSC generation (61,62). In agreement with that, we found that transient depletion of Rif1 significantly enhances reprogramming. Our result supports previous reports that repressive chromatin marks, such as H3K9 and DNA methylation (77,78), are barriers of somatic cell reprogramming. It is also consistent with the finding that depletion of other retrotransposon repressors such as Trim28, Setdb1 and Chaf1a/1b can promote iPSCs derivation (63,65).

DATA AVAILABILITY

The datasets supporting the conclusions of this article are available in the GEO repository, GSE98256.

SUPPLEMENTARY DATA

Supplementary Data are available at NAR Online.

ACKNOWLEDGEMENTS

We thank Dr Shaun Cowley, Dr Masaki Okano and Dr Dongyi Xu for providing the E14-CreER ESCs, Dnmt-TKO ESCs and Rif1 cDNA. We thank the NIEHS Epigenomics, Bioinformatics, Flow Cytometry, Viral Vector and Imaging core facility for assistance with various techniques and experiments.

Author Contributions **:** P.L., G.H. conceived the study. P.L., L.W., J.L., M.T., Y.Q. carried out the experiments. B.B., J.W. analyzed the data. J.M.W., P.A.W., G.H. interpreted the data. P.L., G.H. wrote the manuscript.

FUNDING

Intramural Research Program of the NIH (in part); National Institute of Environmental Health Sciences (NIEHS) [Z01ES102745 to GH, Z01ES101965 to PAW]. Funding for open acces charge: NIEHS [Z01ES102745].

Conflict of interest statement. None declared.

REFERENCES

1. Friedli,M. and Trono,D. (2015) The developmental control of transposable elements and the evolution of higher species. *Annu. Rev. Cell Dev. Biol.*, **31**, 429–451.
2. Groh,S. and Schotta,G. (2017) Silencing of endogenous retroviruses by heterochromatin. *Cell Mol. Life Sci.*, **74**, 2055–2065.
3. Molaro,A. and Malik,H.S. (2016) Hide and seek: how chromatin-based pathways silence retroelements in the mammalian germline. *Curr. Opin. Genet. Dev.*, **37**, 51–58.
4. Schlesinger,S. and Goff,S.P. (2015) Retroviral transcriptional regulation and embryonic stem cells: war and peace. *Mol. Cell. Biol.*, **35**, 770–777.
5. Stocking,C. and Kozak,C.A. (2008) Murine endogenous retroviruses. *Cell Mol. Life Sci.*, **65**, 3383–3398.

6. Garcia-Perez,J.L., Widmann,T.J. and Adams,I.R. (2016) The impact of transposable elements on mammalian development. *Development*, **143**, 4101–4114.
7. Gerdes,P., Richardson,S.R., Mager,D.L. and Faulkner,G.J. (2016) Transposable elements in the mammalian embryo: pioneers surviving through stealth and service. *Genome Biol.*, **17**, 100.
8. Cheng,B., Ren,X. and Kerppola,T.K. (2014) KAP1 represses differentiation-inducible genes in embryonic stem cells through cooperative binding with PRC1 and derepresses pluripotency-associated genes. *Mol. Cell. Biol.*, **34**, 2075–2091.
9. Leeb,M., Pasini,D., Novatchkova,M., Jaritz,M., Helin,K. and Wutz,A. (2010) Polycomb complexes act redundantly to repress genomic repeats and genes. *Genes Dev.*, **24**, 265–276.
10. Bilodeau,S., Kagey,M.H., Frampton,G.M., Rahl,P.B. and Young,R.A. (2009) SetDB1 contributes to repression of genes encoding developmental regulators and maintenance of ES cell state. *Genes Dev.*, **23**, 2484–2489.
11. Bourc'his,D. and Bestor,T.H. (2004) Meiotic catastrophe and retrotransposon reactivation in male germ cells lacking Dnmt3L. *Nature*, **431**, 96–99.
12. Walsh,C.P., Chaillet,J.R. and Bestor,T.H. (1998) Transcription of IAP endogenous retroviruses is constrained by cytosine methylation. *Nat. Genet.*, **20**, 116–117.
13. Karimi,M.M., Goyal,P., Maksakova,I.A., Bilenky,M., Leung,D., Tang,J.X., Shinkai,Y., Mager,D.L., Jones,S., Hirst,M. *et al.* (2011) DNA methylation and SETDB1/H3K9me3 regulate predominantly distinct sets of genes, retroelements, and chimeric transcripts in mESCs. *Cell Stem Cell*, **8**, 676–687.
14. Matsui,T., Leung,D., Miyashita,H., Maksakova,I.A., Miyachi,H., Kimura,H., Tachibana,M., Lorincz,M.C. and Shinkai,Y. (2010) Proviral silencing in embryonic stem cells requires the histone methyltransferase ESET. *Nature*, **464**, 927–931.
15. Maksakova,I.A., Thompson,P.J., Goyal,P., Jones,S.J., Singh,P.B., Karimi,M.M. and Lorincz,M.C. (2013) Distinct roles of KAP1, HP1 and G9a/GLP in silencing of the two-cell-specific retrotransposon MERVL in mouse ES cells. *Epigenetics Chromatin*, **6**, 15.
16. Bulut-Karslioglu,A., De La Rosa-Velazquez,I.A., Ramirez,F., Barenboim,M., Onishi-Seebacher,M., Arand,J., Galan,C., Winter,G.E., Engist,B., Gerle,B. *et al.* (2014) Suv39h-dependent H3K9me3 marks intact retrotransposons and silences LINE elements in mouse embryonic stem cells. *Mol. Cell*, **55**, 277–290.
17. Walter,M., Teissandier,A., Perez-Palacios,R. and Bourc'his,D. (2016) An epigenetic switch ensures transposon repression upon dynamic loss of DNA methylation in embryonic stem cells. *Elife*, **5**, e11418
18. Macfarlan,T.S., Gifford,W.D., Agarwal,S., Driscoll,S., Lettieri,K., Wang,J., Andrews,S.E., Franco,L., Rosenfeld,M.G., Ren,B. *et al.* (2011) Endogenous retroviruses and neighboring genes are coordinately repressed by LSD1/KDM1A. *Genes Dev.*, **25**, 594–607.
19. Reichmann,J., Crichton,J.H., Madej,M.J., Taggart,M., Gautier,P., Garcia-Perez,J.L., Meehan,R.R. and Adams,I.R. (2012) Microarray analysis of LTR retrotransposon silencing identifies Hdac1 as a regulator of retrotransposon expression in mouse embryonic stem cells. *PLoS Comput. Biol.*, **8**, e1002486.
20. Rowe,H.M., Jakobsson,J., Mesnard,D., Rougemont,J., Reynard,S., Aktas,T., Maillard,P.V., Layard-Liesching,H., Verp,S., Marquis,J. *et al.* (2010) KAP1 controls endogenous retroviruses in embryonic stem cells. *Nature*, **463**, 237–240.
21. Wolf,D. and Goff,S.P. (2007) TRIM28 mediates primer binding site-targeted silencing of murine leukemia virus in embryonic cells. *Cell*, **131**, 46–57.
22. Wolf,D. and Goff,S.P. (2009) Embryonic stem cells use ZFP809 to silence retroviral DNAs. *Nature*, **458**, 1201–1204.
23. Schlesinger,S., Lee,A.H., Wang,G.Z., Green,L. and Goff,S.P. (2013) Proviral silencing in embryonic cells is regulated by Yin Yang 1. *Cell Rep.*, **4**, 50–58.
24. Hayashi,M., Maehara,K., Harada,A., Semba,Y., Kudo,K., Takahashi,H., Oki,S., Meno,C., Ichiyanagi,K., Akashi,K. *et al.* (2016) Chd5 Regulates MuERV-L/MERVL Expression in Mouse Embryonic Stem Cells Via H3K27me3 Modification and Histone H3.1/H3.2. *J. Cell Biochem.*, **117**, 780–792.
25. Yang,B.X., El Farran,C.A., Guo,H.C., Yu,T., Fang,H.T., Wang,H.F., Schlesinger,S., Seah,Y.F., Goh,G.Y., Neo,S.P. *et al.* (2015) Systematic identification of factors for provirus silencing in embryonic stem cells. *Cell*, **163**, 230–245.
26. Hardy,C.F., Sussel,L. and Shore,D. (1992) A RAP1-interacting protein involved in transcriptional silencing and telomere length regulation. *Genes Dev.*, **6**, 801–814.
27. Buonomo,S.B. (2010) Heterochromatin DNA replication and Rif1. *Exp. Cell Res.*, **316**, 1907–1913.
28. Chapman,J.R., Barral,P., Vannier,J.B., Borel,V., Steger,M., Tomas-Loba,A., Sartori,A.A., Adams,I.R., Batista,F.D. and Boulton,S.J. (2013) RIF1 is essential for 53BP1-dependent nonhomologous end joining and suppression of DNA double-strand break resection. *Mol. Cell*, **49**, 858–871.
29. Di Virgilio,M., Callen,E., Yamane,A., Zhang,W., Jankovic,M., Gitlin,A.D., Feldhahn,N., Resch,W., Oliveira,T.Y., Chait,B.T. *et al.* (2013) Rif1 prevents resection of DNA breaks and promotes immunoglobulin class switching. *Science*, **339**, 711–715.
30. Escribano-Diaz,C., Orthwein,A., Fradet-Turcotte,A., Xing,M., Young,J.T., Tkac,J., Cook,M.A., Rosebrock,A.P., Munro,M., Canny,M.D. *et al.* (2013) A cell cycle-dependent regulatory circuit composed of 53BP1-RIF1 and BRCA1-CtIP controls DNA repair pathway choice. *Mol. Cell*, **49**, 872–883.
31. Silverman,J., Takai,H., Buonomo,S.B., Eisenhaber,F. and de Lange,T. (2004) Human Rif1, ortholog of a yeast telomeric protein, is regulated by ATM and 53BP1 and functions in the S-phase checkpoint. *Genes Dev.*, **18**, 2108–2119.
32. Xu,D., Muniandy,P., Leo,E., Yin,J., Thangavel,S., Shen,X., Ii,M., Agama,K., Guo,R., Fox,D. 3rd *et al.* (2010) Rif1 provides a new DNA-binding interface for the Bloom syndrome complex to maintain normal replication. *EMBO J.*, **29**, 3140–3155.
33. Zimmermann,M., Lottersberger,F., Buonomo,S.B., Sfeir,A. and de Lange,T. (2013) 53BP1 regulates DSB repair using Rif1 to control 5' end resection. *Science*, **339**, 700–704.
34. Cornacchia,D., Dileep,V., Quivy,J.P., Foti,R., Tili,F., Santarella-Mellwig,R., Antony,C., Almouzni,G., Gilbert,D.M. and Buonomo,S.B. (2012) Mouse Rif1 is a key regulator of the replication-timing programme in mammalian cells. *EMBO J.*, **31**, 3678–3690.
35. Hayano,M., Kanoh,Y., Matsumoto,S., Renard-Guillet,C., Shirahige,K. and Masai,H. (2012) Rif1 is a global regulator of timing of replication origin firing in fission yeast. *Genes Dev.*, **26**, 137–150.
36. Yamazaki,S., Ishii,A., Kanoh,Y., Oda,M., Nishito,Y. and Masai,H. (2012) Rif1 regulates the replication timing domains on the human genome. *EMBO J.*, **31**, 3667–3677.
37. Dan,J., Liu,Y., Liu,N., Chiourea,M., Okuka,M., Wu,T., Ye,X., Mou,C., Wang,L., Wang,L. *et al.* (2014) Rif1 maintains telomere length homeostasis of ESCs by mediating heterochromatin silencing. *Dev. Cell*, **29**, 7–19.
38. Hu,G., Kim,J., Xu,Q., Leng,Y., Orkin,S.H. and Elledge,S.J. (2009) A genome-wide RNAi screen identifies a new transcriptional module required for self-renewal. *Genes Dev.*, **23**, 837–848.
39. Loh,Y.H., Wu,Q., Chew,J.L., Vega,V.B., Zhang,W., Chen,X., Bourque,G., George,J., Leong,B., Liu,J. *et al.* (2006) The Oct4 and Nanog transcription network regulates pluripotency in mouse embryonic stem cells. *Nat. Genet.*, **38**, 431–440.
40. Buonomo,S.B., Wu,Y., Ferguson,D. and de Lange,T. (2009) Mammalian Rif1 contributes to replication stress survival and homology-directed repair. *J. Cell Biol.*, **187**, 385–398.
41. Zheng,X., Dumitru,R., Lackford,B.L., Freudenberg,J.M., Singh,A.P., Archer,T.K., Jothi,R. and Hu,G. (2012) Cnot1, Cnot2, and Cnot3 maintain mouse and human ESC identity and inhibit extraembryonic differentiation. *Stem Cells*, **30**, 910–922.
42. Borkent,M., Bennett,B.D., Lackford,B., Bar-Nur,O., Brumbaugh,J., Wang,L., Du,Y., Fargo,D.C., Apostolou,E., Cheloufi,S. *et al.* (2016) A Serial shRNA Screen for Roadblocks to Reprogramming Identifies the Protein Modifier SUMO2. *Stem Cell Rep.*, **6**, 704–716.
43. Méndez,J. and Stillman,B. (2000) Chromatin association of human origin recognition complex, cdc6, and minichromosome maintenance proteins during the cell cycle: assembly of prereplication complexes in late mitosis. *Mol. Cell. Biol.*, **20**, 8602–8612.
44. Wang,L., Du,Y., Ward,J.M., Shimbo,T., Lackford,B., Zheng,X., Miao,Y.L., Zhou,B., Han,L., Fargo,D.C. *et al.* (2014) INO80 facilitates pluripotency gene activation in embryonic stem cell self-renewal, reprogramming, and blastocyst development. *Cell Stem Cell*, **14**, 575–591.

45. Buenrostro,J.D., Wu,B., Chang,H.Y. and Greenleaf,W.J. (2015) ATAC-seq: a method for assaying chromatin accessibility genome-wide. *Curr. Protoco. Mol. Biol.*, **109**, 21–29.
46. Liu,X., Gao,Q., Li,P., Zhao,Q., Zhang,J., Li,J., Koseki,H. and Wong,J. (2013) UHRF1 targets DNMT1 for DNA methylation through cooperative binding of hemi-methylated DNA and methylated H3K9. *Nat. Commun.*, **4**, 1563.
47. Sommer,C.A., Stadtfeld,M., Murphy,G.J., Hochedlinger,K., Kotton,D.N. and Mostoslavsky,G. (2009) Induced pluripotent stem cell generation using a single lentiviral stem cell cassette. *Stem Cells*, **27**, 543–549.
48. Xue,Z., Huang,K., Cai,C., Cai,L., Jiang,C.Y., Feng,Y., Liu,Z., Zeng,Q., Cheng,L., Sun,Y.E. *et al.* (2013) Genetic programs in human and mouse early embryos revealed by single-cell RNA sequencing. *Nature*, **500**, 593–597.
49. Macfarlan,T.S., Gifford,W.D., Driscoll,S., Lettieri,K., Rowe,H.M., Bonanomi,D., Firth,A., Singer,O., Trono,D. and Pfaff,S.L. (2012) Embryonic stem cell potency fluctuates with endogenous retrovirus activity. *Nature*, **487**, 57–63.
50. Rowe,H.M., Kapopoulou,A., Corsinotti,A., Fasching,L., Macfarlan,T.S., Tarabay,Y., Viville,S., Jakobsson,J., Pfaff,S.L. and Trono,D. (2013) TRIM28 repression of retrotransposon-based enhancers is necessary to preserve transcriptional dynamics in embryonic stem cells. *Genome Res.***3**, 452–461.
51. Mozzetta,C., Pontis,J., Fritsch,L., Robin,P., Portoso,M., Proux,C., Margueron,R. and Ait-Si-Ali,S. (2014) The histone H3 lysine 9 methyltransferases G9a and GLP regulate polycomb repressive complex 2-mediated gene silencing. *Mol. Cell*, **53**, 277–289.
52. Brinkman,A.B., Gu,H., Bartels,S.J., Zhang,Y., Matarese,F., Simmer,F., Marks,H., Bock,C., Gnirke,A., Meissner,A. *et al.* (2012) Sequential ChIP-bisulfite sequencing enables direct genome-scale investigation of chromatin and DNA methylation cross-talk. *Genome Res.*, **22**, 1128–1138.
53. De Iaco,A., Planet,E., Coluccio,A., Verp,S., Duc,J. and Trono,D. (2017) DUX-family transcription factors regulate zygotic genome activation in placental mammals. *Nat. Genet.*, **49**, 941–945.
54. Hendrickson,P.G., Dorais,J.A., Grow,E.J., Whiddon,J.L., Lim,J.W., Wike,C.L., Weaver,B.D., Pflueger,C., Emery,B.R., Wilcox,A.L. *et al.* (2017) Conserved roles of mouse DUX and human DUX4 in activating cleavage-stage genes and MERVL/HERVL retrotransposons. *Nat. Genet.*, **49**, 925–934.
55. Whiddon,J.L., Langford,A.T., Wong,C.J., Zhong,J.W. and Tapscott,S.J. (2017) Conservation and innovation in the DUX4-family gene network. *Nat. Genet.*, **49**, 935–940.
56. Foti,R., Gnan,S., Cornacchia,D., Dileep,V., Bulut-Karslioglu,A., Diehl,S., Buness,A., Klein,F.A., Huber,W., Johnstone,E. *et al.* (2016) Nuclear architecture organized by Rif1 underpins the replication-timing program. *Mol. Cell*, **61**, 260–273.
57. Buenrostro,J.D., Giresi,P.G., Zaba,L.C., Chang,H.Y. and Greenleaf,W.J. (2013) Transposition of native chromatin for fast and sensitive epigenomic profiling of open chromatin, DNA-binding proteins and nucleosome position. *Nat. Methods*, **10**, 1213–1218.
58. Hagarman,J.A., Motley,M.P., Kristjansdottir,K. and Soloway,P.D. (2013) Coordinate regulation of DNA methylation and H3K27me3 in mouse embryonic stem cells. *PLoS One*, **8**, e53880.
59. Elsasser,S.J., Noh,K.M., Diaz,N., Allis,C.D. and Banaszynski,L.A. (2015) Histone H3.3 is required for endogenous retroviral element silencing in embryonic stem cells. *Nature*, **522**, 240–244.
60. Sreesankar,E., Senthilkumar,R., Bharathi,V., Mishra,R.K. and Mishra,K. (2012) Functional diversification of yeast telomere associated protein, Rif1, in higher eukaryotes. *BMC Genomics*, **13**, 255.
61. Friedli,M., Turelli,P., Kapopoulou,A., Rauwel,B., Castro-Diaz,N., Rowe,H.M., Ecco,G., Unzu,C., Planet,E., Lombardo,A. *et al.* (2014) Loss of transcriptional control over endogenous retroelements during reprogramming to pluripotency. *Genome Res.*, **24**, 1251–1259.
62. Ohnuki,M., Tanabe,K., Sutou,K., Teramoto,I., Sawamura,Y., Narita,M., Nakamura,M., Tokunaga,Y., Nakamura,M., Watanabe,A. *et al.* (2014) Dynamic regulation of human endogenous retroviruses mediates factor-induced reprogramming and differentiation potential. *Proc. Natl. Acad. Sci. U.S.A.*, **111**, 12426–12431.
63. Cheloufi,S., Elling,U., Hopfgartner,B., Jung,Y.L., Murn,J., Ninova,M., Hubmann,M., Badeaux,A.I., Euong Ang,C., Tenen,D. *et al.* (2015) The histone chaperone CAF-1 safeguards somatic cell identity. *Nature*, **528**, 218–224.
64. Onder,T.T., Kara,N., Cherry,A., Sinha,A.U., Zhu,N., Bernt,K.M., Cahan,P., Marcarci,B.O., Unternaehrer,J., Gupta,P.B. *et al.* (2012) Chromatin-modifying enzymes as modulators of reprogramming. *Nature*, **483**, 598–602.
65. Miles,D.C., de Vries,N.A., Gisler,S., Lieftink,C., Akhtar,W., Gogola,E., Pawlitzky,I., Hulsman,D., Tanger,E., Koppens,M. *et al.* (2017) TRIM28 is an epigenetic barrier to induced pluripotent stem cell reprogramming. *Stem Cells*, **35**, 147–157.
66. Smith,J.S., Caputo,E. and Boeke,J.D. (1999) A genetic screen for ribosomal DNA silencing defects identifies multiple DNA replication and chromatin-modulating factors. *Mol. Cell. Biol.*, **19**, 3184–3197.
67. Zofall,M., Smith,D.R., Mizuguchi,T., Dhakshnamoorthy,J. and Grewal,S.I. (2016) Taz1-shelterin promotes facultative heterochromatin assembly at chromosome-internal sites containing late replication origins. *Mol. Cell*, **62**, 862–874.
68. Toteva,T., Mason,B., Kanoh,Y., Brogger,P., Green,D., Verhein-Hansen,J., Masai,H. and Thon,G. (2017) Establishment of expression-state boundaries by Rif1 and Taz1 in fission yeast. *Proc. Natl. Acad. Sci. U.S.A.*, **114**, 1093–1098.
69. Sreesankar,E., Bharathi,V., Mishra,R.K. and Mishra,K. (2015) Drosophila Rif1 is an essential gene and controls late developmental events by direct interaction with PP1-87B. *Sci. Rep.*, **5**, 10679.
70. Levis,R.W., Ganesan,R., Houtchens,K., Tolar,L.A. and Sheen,F.M. (1993) Transposons in place of telomeric repeats at a Drosophila telomere. *Cell*, **75**, 1083–1093.
71. Vermeulen,M., Eberl,H.C., Matarese,F., Marks,H., Denissov,S., Butter,F., Lee,K.K., Olsen,J.V., Hyman,A.A., Stunnenberg,H.G. *et al.* (2010) Quantitative interaction proteomics and genome-wide profiling of epigenetic histone marks and their readers. *Cell*, **142**, 967–980.
72. Sukackaite,R., Cornacchia,D., Jensen,M.R., Mas,P.J., Blackledge,M., Enervald,E., Duan,G., Auchynnikava,T., Kohn,M., Hart,D.J. *et al.* (2017) Mouse Rif1 is a regulatory subunit of protein phosphatase 1 (PP1). *Sci. Rep.*, **7**, 2119.
73. Hatanaka,Y., Inoue,K., Oikawa,M., Kamimura,S., Ogonuki,N., Kodama,E.N., Ohkawa,Y., Tsukada,Y. and Ogura,A. (2015) Histone chaperone CAF-1 mediates repressive histone modifications to protect preimplantation mouse embryos from endogenous retrotransposons. *Proc. Natl. Acad. Sci. U.S.A.*, **112**, 14641–14646.
74. Zalzman,M., Falco,G., Sharova,L.V., Nishiyama,A., Thomas,M., Lee,S.L., Stagg,C.A., Hoang,H.G., Yang,H.T., Indig,F.E. *et al.* (2010) Zscan4 regulates telomere elongation and genomic stability in ES cells. *Nature*, **464**, 858–863.
75. Akiyama,T., Xin,L., Oda,M., Sharov,A.A., Amano,M., Piao,Y., Cadet,J.S., Dudekula,D.B., Qian,Y., Wang,W. *et al.* (2015) Transient bursts of Zscan4 expression are accompanied by the rapid derepression of heterochromatin in mouse embryonic stem cells. *DNA Res.*, **22**, 307–318.
76. Amano,T., Hirata,T., Falco,G., Monti,M., Sharova,L.V., Amano,M., Sheer,S., Hoang,H.G., Piao,Y., Stagg,C.A. *et al.* (2013) Zscan4 restores the developmental potency of embryonic stem cells. *Nat. Commun.*, **4**, 1966.
77. Chen,J., Liu,H., Liu,J., Qi,J., Wei,B., Yang,J., Liang,H., Chen,Y., Chen,J., Wu,Y. *et al.* (2013) H3K9 methylation is a barrier during somatic cell reprogramming into iPSCs. *Nat. Genet.*, **45**, 34–42.
78. Mikkelsen,T.S., Hanna,J., Zhang,X., Ku,M., Wernig,M., Schorderet,P., Bernstein,B.E., Jaenisch,R., Lander,E.S. and Meissner,A. (2008) Dissecting direct reprogramming through integrative genomic analysis. *Nature*, **454**, 49–55.